Original Article

AOSPINE NORTH AMERICA

Global Spine Journal
2018, Vol. 8(8) 847-859

DOI: 10.1177/2192568218779988
journals.sagepub.com/home/gsj
SAGE

A Comparison of Two Ovine Lumbar Intervertebral Disc Injury Models for the Evaluation and Development of Novel Regenerative Therapies

Chris D. Daly, MBBS, MPhil, PhD[1,2], Peter Ghosh, DSc, PhD, FRSC[1,3], Tanya Badal, MSc[4], Ronald Shimmon, PhD[4], Graham Jenkin, PhD[1], David Oehme, MBBS, PhD, FRACS[5], Justin Cooper-White, PhD, BE (Chem)(Hons)[6], Idrees Sher, BAppSc-MRS(DR), BMedSc, MBBS(Hons)[1,2], Ronil V. Chandra, MBBS, FRANZCR[1,2], and Tony Goldschlager, MBBS, PhD, FRACS[1,2]

Abstract

Study Design: Large animal research.

Objective: Lumbar discectomy is the most commonly performed spinal surgical procedure. We investigated 2 large animal models of lumbar discectomy in order to study the regenerative capacity of mesenchymal stem cells following disc injury.

Methods: Twelve adult ewes underwent baseline 3-T magnetic resonance imaging (MRI) followed by lumbar intervertebral disc injury by either drill bit (n = 6) or annulotomy and partial nucleotomy (APN) (n = 6). Necropsies were performed 6 months later. Lumbar spines underwent 3-T and 9.4-T MRI prior to histological, morphological and biochemical analysis.

Results: Drill bit-injured (DBI) and APN-injured discs demonstrated increased Pfirrmann grades relative to uninjured controls ($P < .005$), with no difference between the 2 models. Disc height index loss was greater in the APN group compared with the DBI group ($P < .005$). Gross morphology injury scores were higher in APN than DBI discs ($P < .05$) and both were higher than controls ($P < .005$). Proteoglycan was reduced in the discs of both injury models relative to controls ($P < .005$), but lower in the APN group ($P < .05$). Total collagen of the APN group disc regions was higher than DBI and control discs ($P < .05$). Histology revealed more matrix degeneration, vascular infiltration, and granulation in the APN model.

Conclusion: Although both models produced disc degeneration, the APN model better replicated the pathobiology of human discs postdiscectomy. We therefore concluded that the APN model was a more appropriate model for the investigation of the regenerative capacity of mesenchymal stem cells administered postdiscectomy.

Keywords

animal model, intervertebral disc, discectomy, regeneration

Introduction

Lower back pain causes more global disability than any other condition worldwide.[1] Lower back pain commonly results from degenerative lumbar disc disease causing discogenic pain.[2] Lumbar disc degeneration is a complex process manifested by changes in cellular, matrix, endplate, and the neurovascular components of the intervertebral disc. Intervertebral disc herniation is a common outcome of lumbar disc degeneration, while lumbar discectomy is the most commonly performed

[1] Monash University, Clayton, Victoria, Australia
[2] Monash Medical Centre, Clayton, Victoria, Australia
[3] Proteobioactives, Pty Ltd, Sydney, New South Wales, Australia
[4] University of Technology Sydney, Broadway, New South Wales, Australia
[5] St Vincent's Hospital, Fitzroy, Victoria, Australia
[6] University of Queensland, St Lucia, Queensland, Australia

Corresponding Author:
Chris D. Daly, The Ritchie Centre, Hudson Institute of Medical Research, Monash University, 246 Clayton Road, Clayton, Victoria, 3168, Australia.
Email: chrisddaly@gmail.com

spinal surgical procedure.[3] Lumbar discectomy successfully treats radicular symptoms associated with neural compression in more than 80% of patients.[4] However, the procedure fails to address the underlying pathophysiology of intervertebral disc degeneration responsible for the syndrome. Moreover, following lumbar discectomy up to one-third of patients report low back pain.[5] In addition, up to 18% of patients experience recurrent disc herniation[6] with 12% undergoing reoperation within 4 years.[7] Ultimately, 40% of these patients will undergo spinal fusion.[7]

Given the significant disease burden resulting from disc degeneration and lower back pain numerous animal models have been developed to further understand the pathobiology of disc degeneration and examine potential modalities for its treatment.[8] There are, however, relatively few reports of large animal models of lumbar discectomy.[9-12] Given the clinical ubiquity of discectomy, the inherent anatomical challenges to disc repair and the opportunity presented to initiate regenerative therapy at the time of surgical intervention, we sought to develop a suitable large animal model of discectomy that could be used to evaluate potential tissue regenerative therapies, such as transplantation of stem cells.

Limited annular injury to ovine discs have been widely used to generate a model of disc degeneration.[13-15] The ovine species has also been used to test implant devices and in the preclinical investigation of cellular therapies to support spinal fusion and disc reconstitution.[9,16-18] Ovine discs, like human discs, undergo chondroid metaplasia with skeletal maturation,[19] because of the loss of their notochordal cell remnants.[19,20] Additionally, the ovine disc is closer in size and cellular phenotype[20] to the human intervertebral disc than small animal models, important characteristics given the nutritional limitations associated with the central regions of the disc. Furthermore, despite its quadrupedal conformation, the sheep spine has been shown to exhibit significant biomechanical similarities to the human spine.[21]

We have previously described the use of an ovine annulotomy and partial nucleotomy (APN) model for investigation of the potential of mesenchymal progenitor cells (MPCs) formulated with the pharmaceutical agent, pentosan polysulfate (PPS), embedded in a biodegradable gelatin scaffold to promote intervertebral disc regeneration following lumbar discectomy in a pilot study.[9] In this APN model, a full-thickness 3×5 mm annulotomy was performed with a scalpel blade and 200 mg of annular and nuclear tissue removed with a pituitary rongeur. PPS was used as it was known to enhance MPC viability and promote their differentiation to a chondrogenic phenotype whilst also inhibiting osteogenesis.[22] Our pilot study demonstrated the feasibility of the modified APN model and provided positive outcomes on the efficacy of the MPC + PPS formulation. However, prior to further investigations of other potential therapeutic modalities of lumbar disc repair that required the use of a liquid hydrogel, we sought to determine the most appropriate large animal model for such applications.

An earlier publication by Zhang et al[23] reported that disc degeneration could be induced in goat lumbar discs by using a drill bit to penetrate the annulus fibrosus (AF) through to the nucleus pulposus (NP). Using a subjective histological grading system, this model was reported to provide more reliable degenerative changes than insertion of a horizontal surgical blade along the same path. In principle, the Zhang et al[23] model offers advantages in facilitating the injection of regenerative liquid hydrogels/cell combinations into the disc without the use of a solid scaffold, which was a requirement of using the Oehme discectomy model.[9] However, the study of Zhang et al[23] was performed in goats and did not include biochemical analysis of the injured intervertebral discs, thereby limiting the ability to directly compare these 2 models directly.

The drill bit injury (DBI) model produces injury of both the annulus and nucleus. We hypothesized that modification of this model by increasing the depth of penetration to the midpoint of the nucleus pulposus and using the maximum drill bit diameter without inducing endplate injury, that is, slightly less than disc height, may provide a readily replicable model of the postdiscectomy intervertebral disc. This model has the advantage of being a single step procedure with a highly standardized annular and nuclear defect. Furthermore, the ovine DBI model could also serve as a model of intervertebral disc herniation, in which nuclear injury is associated with a full thickness annular injury. In the present study, we evaluated the APN and drill bit methods of surgically inducing disc failure using a homogeneous group of adult sheep and monitoring the relative outcomes 6 months later using both subjective and objective methods of assessment.

Material and Methods

Surgical Procedure

With ethics approval from the Monash Medical Centre Animal Ethics Committee and conforming to the Australian code of practice for the care and use of animals for scientific purposes (eighthth edition, 2013), 12 adult (2-4 years of age) Border-Leicester Merino cross-bred ewes underwent preoperative 3-T magnetic resonance imaging (MRI; Siemens Skyra Widebore 3T MRI, Siemens, Erlangen, Germany) under general anesthetic. Ewes were used in this study because of their better temperament than males—castrate or intact. Sheep were raised in open pastures and ambulated freely prior to the trial. All sheep were fasted for 24 hours prior to surgery and anesthetized using intravenous thiopentone (10-15 mg/kg) (Bayer Australia Ltd, Pymble, New South Wales, Australia) followed by intubation and isoflurane inhalation (Pharmachem, Eagle Farm, Queensland, Australia) (2%-3% in oxygen). Sheep were placed in the right lateral position. Local anesthetic (bupivacaine 0.5%) (AstraZeneca Australia, Macquarie Park, New South Wales, Australia) was administered subcutaneously and the L2-3 and L3-4 lumbar intervertebral discs exposed via left lateral retroperitoneal approach, as previously described.[24,25] Intraoperative lateral radiographs (Radlink, Atomscope HF200A, Redondo Beach, CA, USA) were performed to confirm the correct levels. Six sheep underwent microdiscectomy

APN injury, performed by the creation of a 3 mm × 5 mm annular window followed by disc resection using pituitary rongeurs. The disc tissues collected (200.0 ± 3.0 mg) consisted mainly of AF with some NP. The adjacent L1-2 and L4-5 discs served as untreated controls. DBI was performed on the L2/3 and L3/4 intervertebral discs of the remaining 6 sheep using a 3.5-mm Brad point drill bit (Carbatec, Melbourne, Victoria, Australia) with a drill bit stop applied at 12 mm drill bit length (Drill Warehouse, Amazon, Seattle, WA, USA) as described previously.[25]

Following intervertebral disc injury, the wound was closed using a routine layered procedure performed using absorbable sutures (Vicryl, Ethicon, Somerville, NJ, USA). Animals received a fentanyl patch (Duragesic 75 μg/h, Jannsen LLC., North Ryde, New South Wales, Australia) and intravenous paracetamol (Pfizer Ltd, West Ryde, New South Wales, Australia) for postoperative analgesia. Following recovery, animals were returned to the pen with other sheep and allowed free ambulation. Sheep were returned to open pasture 1 week postsurgery.

Necropsy

Six months postsurgery, animals were euthanized by intravenous injection of 150 mg/kg of pentobarbital (Sigma-Aldrich, Castle Hill, New South Wales, Australia). The lumbar spines were then removed en bloc, a segment was isolated from the mid-sacrum to the thoracolumbar junction and transferred to Monash Biomedical Imaging for MRI analysis. Spinal columns were then transected in the horizontal plane through their vertebral bodies, using a band saw, to provide spinal segments consisting of a complete lumbar disc with half of the adjacent vertebral bodies attached. Subsequent gross morphological, biochemical, and histological analysis of discs were undertaken using these spinal segments as described below. Spinal segments containing discs destined for histological analysis were transferred to phosphate buffered formalin.

Radiological Analysis

Using standardized methods, disc height index (DHI) measurements were calculated and recorded by an observer blinded to the treatment regimen, using standard digital processing software (Osiris MD v8.0.2, Pixmeo, Geneva, Switzerland).

Sagittal 3-T (Siemens Skyra Widebore 3T MRI, Siemens, Erlangen, Germany) T2-weighted MRI sequences of the entire lumbar spine explant were obtained for each animal. Axial 9.4-T (Agilent 9.4T MRI Small Animal Scanner Agilent/Varian, Santa Clara, CA, USA) T1 and T2 MRI sequences of the control and intervention lumbar intervertebral discs were taken for each animal. Using sagittal 3-T T2-weighted sequences and 9.4-T T2 sagittal reconstructions (Osiris MD v 8.0.2), 4 blinded observers (a neuroradiologist, neurosurgeon and 2 neurosurgery residents blinded to the treatment regimen) determined the Pfirrmann MRI disc degeneration scores for all lumbar discs.

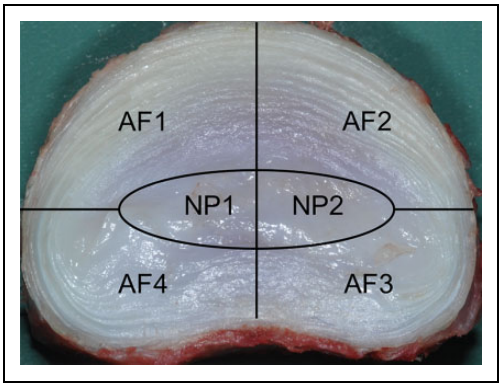

Figure 1. Diagram showing the intervertebral disc segments used for gross morphological and biochemical analysis. AF1 is the site of intervertebral disc injury. NP1 is the region of NP on the injured half of the intervertebral disc. NP2 the complementary half of NP1. AF, annulus fibrosus; NP, nucleus pulposus.

DHI analysis was also performed using the preoperative and 3-T MRI images obtained at necropsy, by an observer blinded to the intervention protocol. The 3-T MRI assessment of the DHI eliminated the potential for parallax error while also producing consistent image quality for all discs.

Gross Morphological Analysis

Lumbar spinal disc segments allocated for gross morphological and biochemical analysis were sectioned in the horizontal (axial) plane using a 100.0 × 25.0 × 2.5 mm blade to provide 2 complementary halves of the disc as shown diagrammatically in Figure 1. High-resolution digital photographs were taken of the exposed complementary surfaces and each region shown in Figure 1 scored by a blinded observer following the criteria in Table 1 described by Daly et al[26] and adapted from the method of Oehme et al.[27]

Biochemical Analysis

After collection of the digital images of discs for morphological analysis all tissue regions shown in Figure 1 were subjected to biochemical analysis. The individual AF and NP from each region were separated from each other and their vertebral attachments by careful dissection using the boundaries shown in Figure 1. Tissues from each region were finely diced, frozen in liquid nitrogen, and powdered in a liquid nitrogen–cooled ball-mill. The powdered tissues were transferred to preweighed Eppendorf vials and weighed, lyophilized, and reweighed to constant weight to determine their anhydrous weights. Triplicate aliquots of the dehydrated tissues were solubilized using a papain digestion buffer (50 mM sodium acetate [pH 6.0]) containing 2 mg/mL papain (Sigma-Aldrich Chemicals, Sydney, New South Wales, Australia) by incubation at 60°C for 16 hours.[28] The digested tissues were centrifuged at 3000 × *g* for 15 minutes and supernatants diluted to standard volumes (the stock digest solution). Aliquots of the stock solution were analyzed for sulfated glycosaminoglycan (S-GAG) (an index of

Table 1. Gross Morphology Criteria Used to Score Segmental Regions (AF and NP) Shown in Figure 1 for Each Disc.[a]

AF Morphological Grades Applied to each AF Quadrant	NP Morphological Grades Applied to Each Half of NP
Grade 0: Normal disc—no annular disruption, discoloration, or hemorrhage	Grade 0: Normal NP—no discoloration or hemorrhage
Grade 1: Minor disruption—annular disruption with minor discoloration and/or hemorrhage	Grade 1: Minor disruption—minor disruption, discoloration, and/or hemorrhage; <10% NP region; minor fissuring and nuclear dehydration may be evident
Grade 2: Moderate disruption—annular disruption with medium discoloration and/or hemorrhage	Grade 2: Moderate disruption—medium disruption, discoloration, and/or hemorrhage; 10%-50% of NP region; moderate fissuring and nuclear dehydration may be evident
Grade 3: Major disruption—annular disruption with significant discoloration and/or hemorrhage	Grade 3: Major disruption—significant disruption, discoloration, and/or hemorrhage; 50%-75% NP region; major fissuring and nuclear dehydration may be evident
Grade 4: Complete disruption—annular disruption with extensive discoloration and/or hemorrhage	Grade 4: Complete disruption—extensive disruption, discoloration, and/or hemorrhage; >75% NP region; extensive fissuring and dehydration may be evident

Abbreviations: AF, annnulus fibrosus; NP, nucleus pulposus.
[a] The sum of all regional scores (AF1, AF2, AF3, AF4, NP1, and NP2) yielded a total disc degeneration score between 0 (normal) and 24 (severely degenerated) for each disc. Table is described in Daly et al[26] and adapted from the method described by Oehme et al.[13]

proteoglycan content) levels using the dimethylmethylene blue (DMMB) assay[29] and hydroxyproline assay (to derive collagen content).[30] The results of biochemical analyses were normalized and were expressed as percentage of tissue dry weight for S-GAG and collagen.

Histological Analysis

The individual disc segments, consisting of the intervertebral disc with attached hemisected vertebral bodies were in 10% neutral buffered formalin for 8 days then stored in 70% ethanol. The volume of vertebral bone was reduced to the growth plate using a fine diamond saw. Prior to paraffin based tissue embedding, decalcification of the remaining vertebral bone was undertaken with multiple changes of 10% formic acid. Coronal paraffin sections of the entire disc segments for the APN sheep and axial sections for the drill injured sheep were cut using a standard rotary microtome and stained using hematoxylin and eosin. Axial sections were taken from the drill injury disc to allow for visualization of the entire DBI tract. The APN-injured discs were only subjected to standard coronal plane sectioning.

Statistical Analysis

All data analyses and storage were performed using Microsoft Excel for Mac (Version 15.33, Microsoft, Redmond, WA, USA) and Prism 7.0c for Mac (GraphPad Software Inc, La Jolla, CA, USA). Parametric data was analyzed using 1-way analysis of variance, and Tukey's multiple comparison test was performed when significant differences in means were observed. Nonparametric data was analyzed using Kruskal-Wallis test of median values followed by Dunn's multiple comparison test. Groups were compared using the 2-tailed Student's t test followed by Mann-Whitney U tests. A P value $<.05$ was considered statistically significant.

Results

Disc Height Index

The APN-injured discs demonstrated significantly greater loss of height than the drill injured and control discs ($P < .005$). However, both the APN and drill injured discs demonstrated greater loss of height than control discs ($P < .005$) (Figure 2A).

Baseline preoperative 3-T MRIs of all animals revealed no evidence of underlying disc degeneration at control or intervention levels (L1/2 to L4/5). Scoring of drill bit– and APN-injured discs demonstrated significantly increased Pfirrmann grades relative to control discs (both $P < .005$); however, there was no significant difference in Pfirrmann grades between the 2 injury groups (Figure 2, A, B, and D).

9.4-T MRI

The horizontal images obtained by 9.4-T MRI allowed ready appreciation of the extent of annular disruption observed in the APN versus drill injured intervertebral discs (Figure 3, B and C) and correlated well with gross morphological observations. However, the 9.4-T MRI Pfirrmann grades were consistent with 3-T grades once sagittal reconstruction and grading was performed (Figure 2, B and D). Significantly increased Pfirrmann grades were observed in the drill- and APN-injured discs compared with control discs ($P < .005$) with no significant difference between the 2 injury models.

Gross Morphology

Gross morphological analysis was completed on a regional basis, with the data presented in Figure 4D showing the aggregate morphological scores. Representative gross morphological digital images are displayed in Figure 4A-C and their respective scores, determined using the criteria described in Table 1 and shown in Figure 4D. Drill injured discs generally demonstrated a more focal annular and nuclear tract injury (Figure 4B), with minimal NP disorganization, in comparison with the APN-injured discs, which showed more widespread

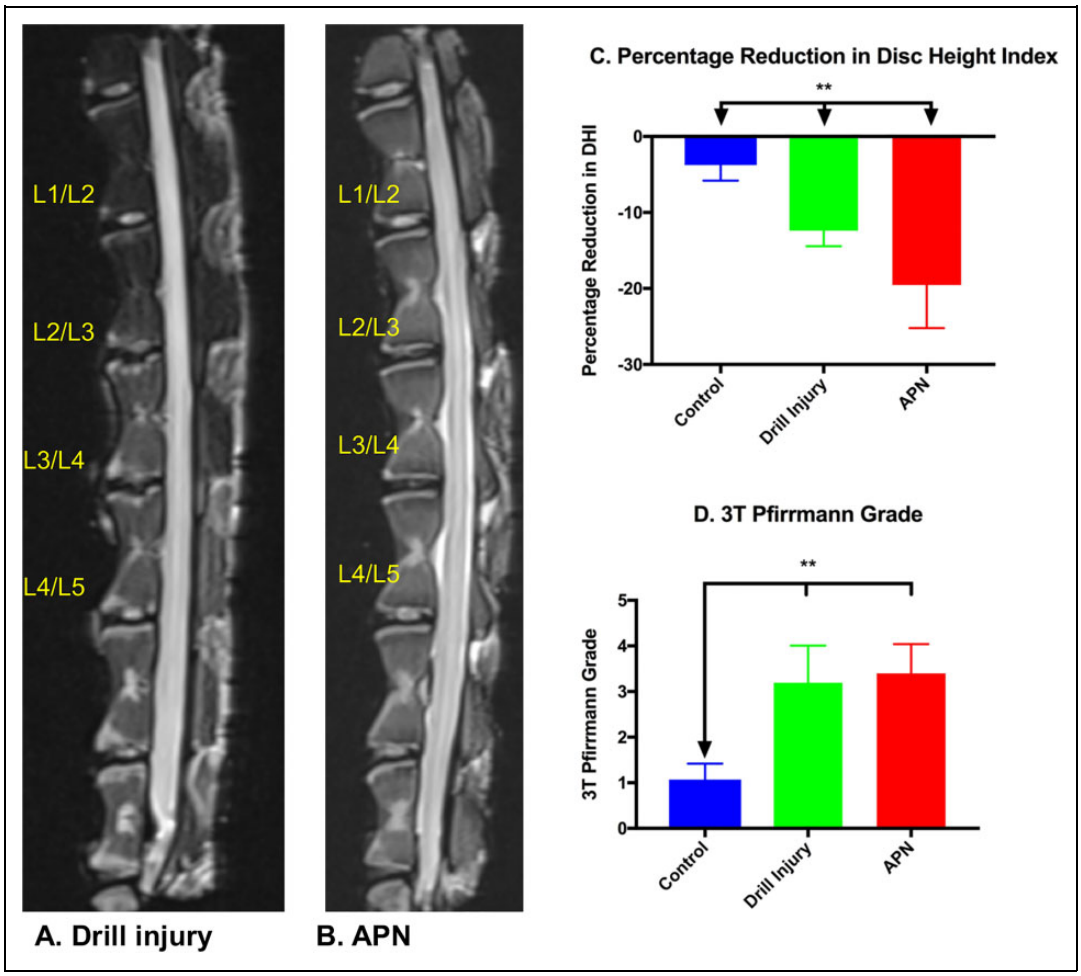

Figure 2. (A) Necropsy sagittal magnetic resonance image (MRI) of the drill injury lumbar spine. (B) APN-injured lumbar spine demonstrating increased Pfirrmann grade in the injured disc (L2/3 and L3/4) relative to control discs (L1/2 and L4/5). (C) Percentage reduction in disc height index. APN and drill injury discs demonstrated significantly greater loss of disc height than control discs. (2D) 3-T Pfirrmann grades: drill bit– and APN-injured discs had significantly increased Pfirrmann grades relative to control discs; however, there was no significant difference in Pfirrmann grades between injury groups. APN, annulotomy and partial nucleotomy. *$P < .05$, **$P < .005$.

changes and blood degradation product staining (Figure 4C). Nonetheless, total disc gross morphological scores were significantly increased in both the drill bit– and APN-injured intervertebral discs relative to control ($P < .005$). APN-injured intervertebral disc gross morphological scores were, however, significantly elevated relative to drill-injured discs ($P < .05$) (Figure 4D).

Proteoglycan Content as Determined by Sulfated-Glycosaminoglycan (S-GAG) Analysis

S-GAG content was significantly reduced in the injured (NP1) (Figure 5A) and contralateral NP region (NP2) (Figure 5B) in both the drill- and APN-injured discs relative to controls ($P < .005$). Furthermore, the APN discs demonstrated significantly less NP1 S-GAG and NP2 S-GAG than the drill injured discs ($P < .005$ and $P < .05$, respectively). This relationship persisted for NP total S-GAG content (Figure 5C). Total disc S-GAG content demonstrated a significant reduction in S-GAG content in the APN-injured disc compared with both control ($P < .005$) and drill-injured discs ($P < .05$) (Figure 5D). There was no significant difference between control and drill-injured total disc S-GAG content.

Collagen Content

The collagen content of the APN injury site AF (AF1) was significantly higher than both the control and drill-injured discs ($P < .05$) (Figure 6A). Furthermore, the drill injury AF1 collagen content was significantly lower than control discs ($P < .05$). The AF adjacent to the injury site (AF4) also demonstrated a significant increase in collagen content in the APN group relative to controls ($P < .01$) (Figure 6B). The nucleus pulposus, both ipsilateral and contralateral to the injury site, demonstrated significantly higher collagen content in the APN-injured disc relative to both the control and drill-injured discs ($P < .005$ and $P < .05$, respectively) (Figure 6, C and D). These differences were also reflected in the total NP and total disc

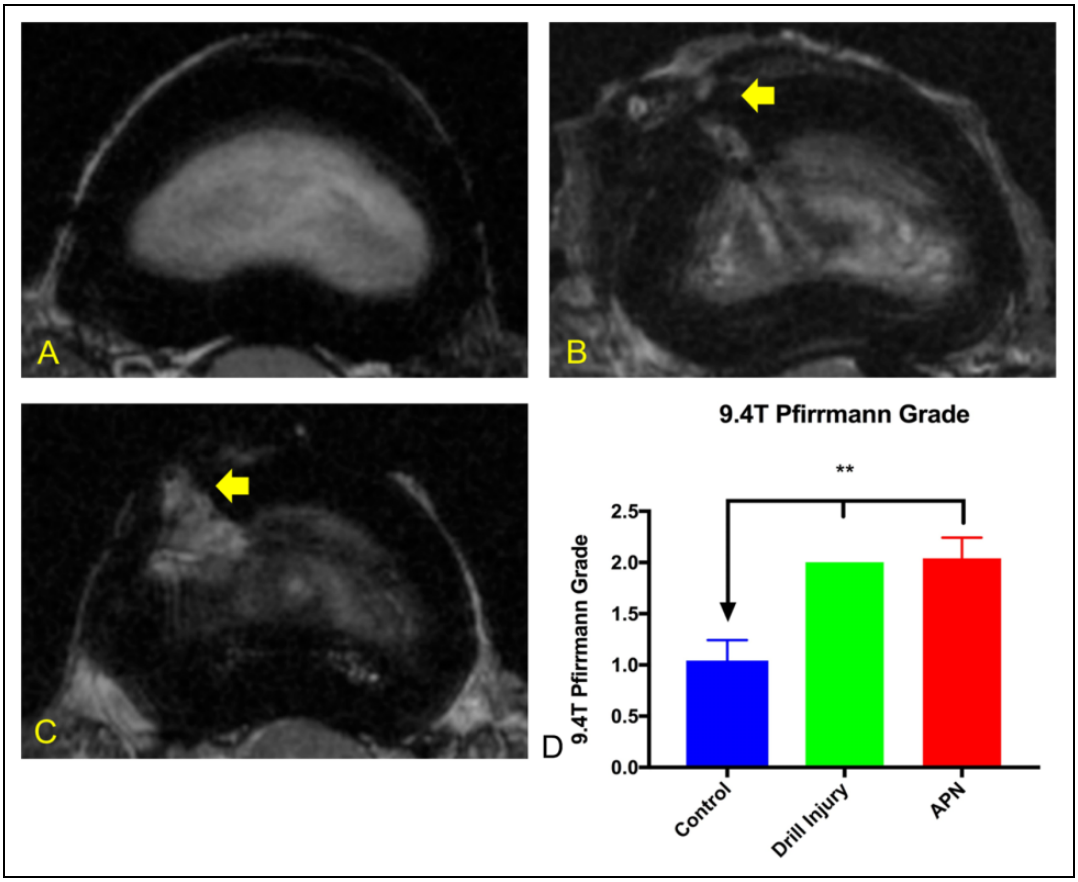

Figure 3. Axial magnetic resonance images (9.4-T) (A) Control disc demonstrating intact AF and hyperintense NP. (B) Drill injury disc demonstrating injury tract (arrow) extending to NP. (C) APN disc demonstrating broader injury tract (arrow) and decreased NP hyperintensity. (D) 9.4-T MRI Pfirrmann grades: drill-injured and APN-injured discs demonstrated significantly higher 9.4-T Pfirrmann grades than control discs with no significant difference between injured groups. AF, annulus fibrosus; NP, nucleus pulposus; APN, annulotomy and partial nucleotomy. *P < .05, **P < .005.

(NP + AF) collagen content of the APN group compared with both the drill-injured and control discs (Figure 6, E and F) (P < .001 and P < .005, respectively).

Histology

Qualititative histological analysis revealed differences between the injury models with regard to the disc ultrastructure and extent of vascular infiltration and granulation tissue deposition. Control discs demonstrate intact annulus fibrosi displaying multiple lamellae abutting the proteoglycan-rich nucleus pulposus (Figures 7A and 8A [axial] and Figures 7B and 8B [coronal]). Axial hematoxylin and eosin–stained slides of drill-injured disc demonstrate the focal nature of the disruption of AF and NP tissues induced by this injury model (Figure 7, C and D). Relatively little vascular infiltration is evident. Reduced proteoglycan content is evident on the drill-injured disc (Figure 8C**)** relative to the control disc (Figure 8A) on the Safranin O and Fast Green–stained slides. The APN-injured disc (Figure 7E) demonstrates extensive disruption of lamellae with deposition of granulation tissue and infiltration within the injury site. High-power microscope images highlighted the extent of vascular proliferation occuring at the injury site of the AF (Figure 7F). Marked reduction in proteolgycan content is also evident at the APN injury site (Figure 8D).

Discussion

The results of the present study demonstrated that both the modified APN injury model originally described by Oehme et al[9] and a modification of the DBI model described by Zhang et al[23] induced degeneration in sheep lumbar discs 6 months following the surgical intervention. Furthermore, as assessed from the disc height indices, gross morphological, biochemical, and histological analyses, the APN injury provoked more extensive degenerative changes in injured discs, than observed with the DBI procedure.

We suggest that the extent and nature of the degenerative changes induced in the discs of each model was determined by the relative magnitude of several time-dependent mechanical and biological events that are known to dictate the pathology of disc degeneration.[31-36] For example, surgical compromise of AF hoop stress tensile function and reduction in NP hydroelasticity would impose an immediate disturbance in the nature of

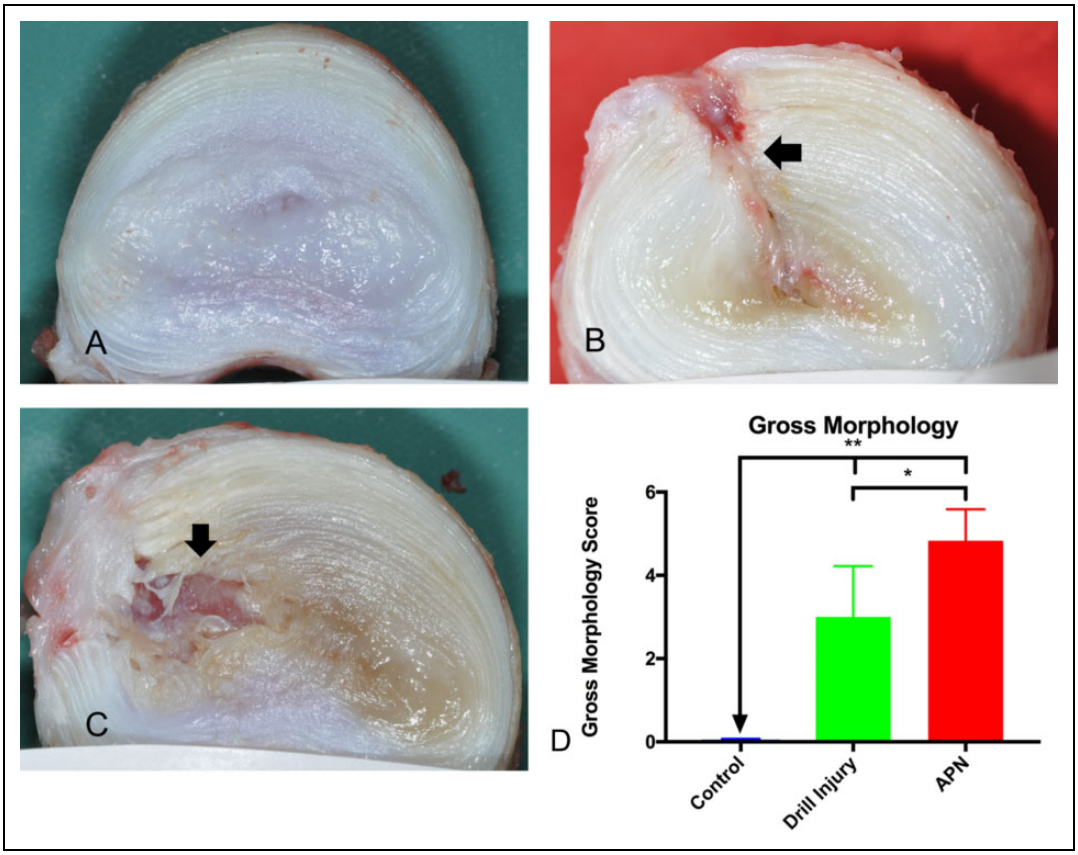

Figure 4. Representative examples of disc gross morphology. (A) Control disc demonstrating intact AF and gelatinous white NP (scored as 0). (B) Drill-injured disc demonstrating injury tract extending to NP (arrow) with discoloration of NP and AF disruption at injury site (scored as 4) (C) APN disc demonstrating broader AF injury (arrow) with extension to NP, loss of NP material, discoloration of NP and AF (scored as 6). (D) Gross morphology scores: drill-injured and APN-injured discs demonstrated significantly higher gross morphology scores than control discs. APN discs demonstrated higher gross morphology scores than drill-injured discs. AF, annulus fibrosus; NP, nucleus pulposus; APN, annulotomy and partial nucleotomy. *$P < .05$, **$P < .005$.

the mechanical stresses acting across the spinal unit and its adjacent structures.[37] A secondary event elicited, would be an inflammation and an early repair response at the site of injury, with proliferation of the capillaries serving the outer AF, accompanied by deposition of granulation and fibrotic tissue within the defect site. Such events have been described in other animal models[13,38-40] and are the sequelae of human disc herniation.[41]

Loss of proteoglycan and its associated water is a relatively early event in the pathophysiology of intervertebral disc degeneration.[31,42] The loss of these matrix components leads to marked changes in the mechanical properties of the intervertebral disc and adjacent structures, as intradiscal pressure is reduced and the ability of the disc to tolerate compressive loading diminishes.[43] Biomechanical studies have demonstrated such changes in the mechanical behavior of discs that were proportional to the size of the annular defects.[35,37,44]

The compromise of AF integrity and loss of NP material initiated in the APN model closely mirrors the clinical condition of symptomatic lumbar intervertebral disc herniation. In the clinical setting, radicular symptoms are caused by herniated intervertebral disc material producing neural compression. This herniated AF and NP, and any additional loose NP, is excised during conventional lumbar microdiscectomy. The creation of a full thickness APN, with removal of 200 mg of annular and nuclear tissue, differentiates this ovine APN model from those recently reported by Shu et al[45] and most other ovine annular injury models in the literature[13,14] in which partial thickness annular incisions are performed. Such models may be more representative of spontaneous intervertebral disc degeneration, in which annular tears are often observed, than the post–lumbar discectomy intervertebral disc.

The model of Zhang et al[23] demonstrated the ability of the DBI to induce disc degeneration 2 months following surgery, confirmed histologically but not biochemically. Furthermore, the degeneration observed histologically did not produce correlative MRI changes such as increased 1.5-T MRI Pfirrmann grades. Many prior studies of the intervertebral disc, including that of Zhang et al,[23] were performed with 1.5-T MRI scanners. With the advance of technology, 3-T MRI scanners are commonly available in the clinical setting and the 9.4-T MRI scanner is now available for preclinical studies. Despite our use of both 3-T and 9.4-T MRI the MRI Pfirrmann grade findings did not directly parallel our histological, biochemical,

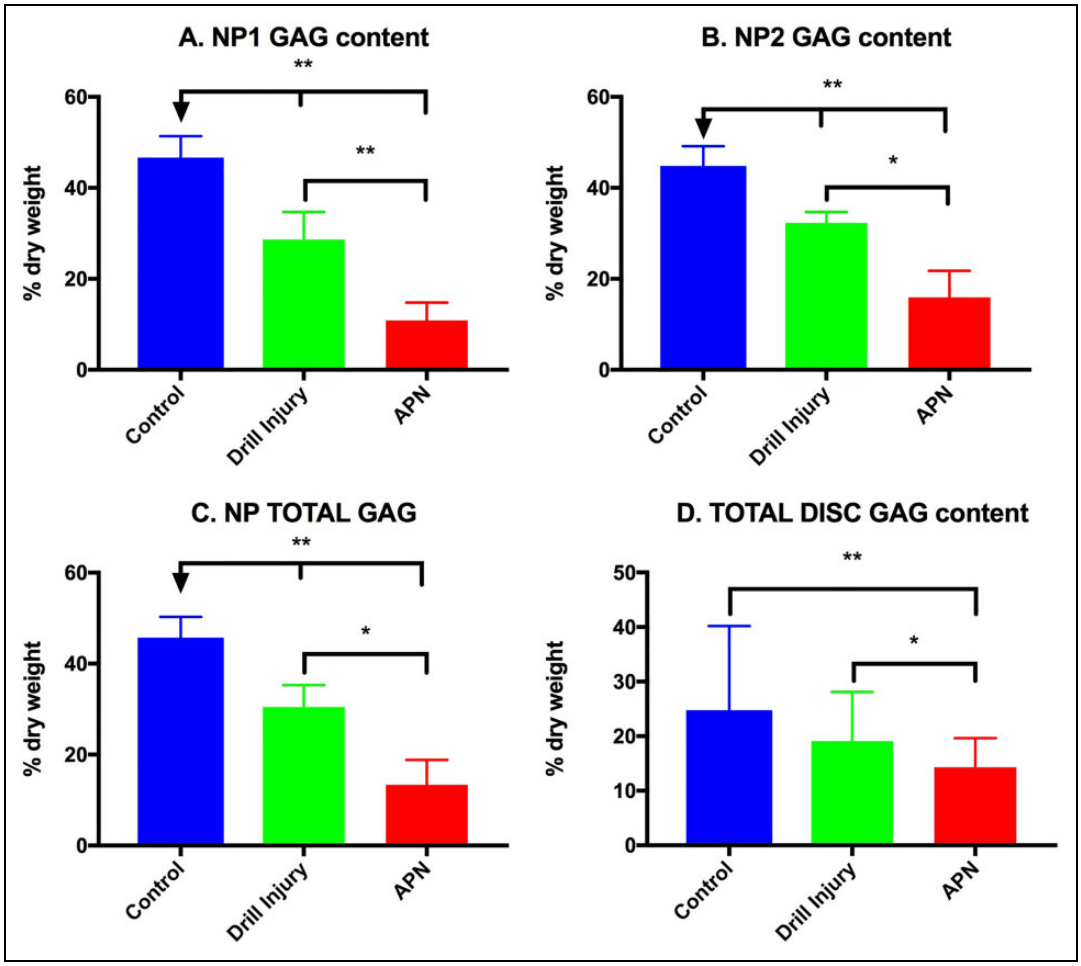

Figure 5. Sulfated glycosaminoglycan (S-GAG) content (% dry weight). (A) NP1 GAG is significantly lower in APN-injured than drill-injured discs, which is in turn less than control discs. (B) NP2 demonstrates the same relationship with APN-injured discs lower than drill-injured discs ($P < .05$), which in turn are less than control discs. (C) NP Total GAG and (D) total disc GAG demonstrates the same series of relationships. APN, annulotomy and partial nucleotomy. *$P < .05$, **$P < .005$.

morphological, and DHI observations. The failure of the MRI Pfirrmann grading system to adequately reflect differences in the extent of intervertebral disc degeneration has been observed for lower resolution 1.5-T and 3-T MRI scanners in both preclinical and clinical studies.[23,26,46-48] We suggest that the discrepancy between the MRI and our other findings may be attributed to the relatively low sensitivity of conventional MRI Pfirrmann grades for detecting subtle degenerative differences relative to other quantitative and semiquantitative modalities. The 9.4-T MRI axial images (Figure 3) provided superior resolution of anatomical detail compared to conventional 1.5-T and 3-T MRI scanners[49]; however, this additional data was not captured in the Pfirrmann grading system when the axial images were converted to the sagittal plane. Advanced quantitative radiological methods, such as $T_{1\rho}$-weighted MRI, may provide a more sensitive method of measuring early intervertebral disc degeneration radiologically using the clinical magnets currently available.[50] Furthermore, our group is investigating novel methods to fully utilize the increased resolution this imaging modality affords.[49]

The increase in collagen observed in the injury site AF and NP of the APN-injured disc reflects the normal tissue response to traumatic injury, with inflammation, capillary invasion, and fibrotic granulation tissue deposition representing key matrix events. The repair tissues that normally accumulate at these early injury sites, consist mainly of type I collagen, and are accompanied by the loss of proteoglycans[33] as was observed for the APN model but not drill bit model. In healthy discs and the early stages of disc degeneration, the chondrocyte-like cells of the NP synthesize predominantly type II collagen.[51] However, as the disc degeneration progresses, these cells undergo a transition and synthesize type I collagen and less proteoglycans.[33] Therefore, it is possible that the endogenous NP cells of the injured discs in the APN model also contributed to the deposition of fibrotic tissue. Additional studies of the collagen subtypes resident in the various regions of the injured discs from the APN model are required to resolve this important question. The observed lack of a significant difference in collagen content between the drill-injured disc and control discs, with the exception of AF1, is indicative of the relatively low-

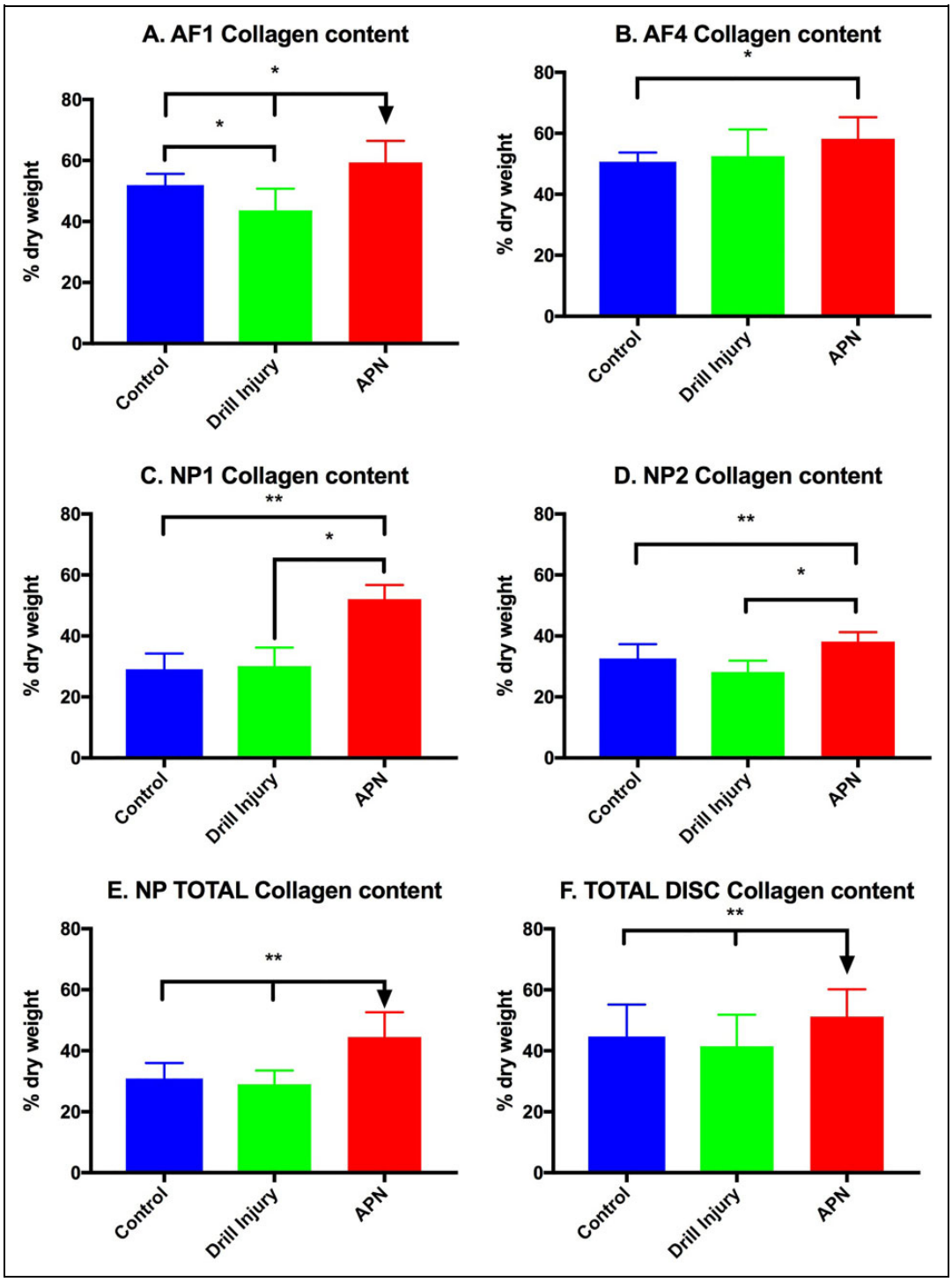

Figure 6. Collagen content (% dry weight). (A) AF1 APN group discs had significantly more collagen than both control and drill-injured discs. (B) AF4 APN group collagen was significantly higher than control discs. (C) NP1 APN group collagen was significantly higher than both control and drill injury collagen. (D) NP2 collagen demonstrated the same pattern. (E) NP total also demonstrated an increase in collagen in the APN group relative to the control group. (F) Total disc collagen was significantly increased in the APN group relative to both control and drill-injured discs. AF, annulus fibrosus; NP, nucleus pulposus; APN, annulotomy and partial nucleotomy. *$P < .05$, **$P < .005$.

grade degeneration changes induced in these tissues by either surgical approach.

As a result of the extended time required to completely decalcify the vertebral bone, the quality of the disc tissue sections was unfortunately unacceptable for quantitative histological scoring. Nevertheless, all histological sections were reviewed qualitatively. On histological examination, vascular invasion was noted in the APN-injured discs that was relatively

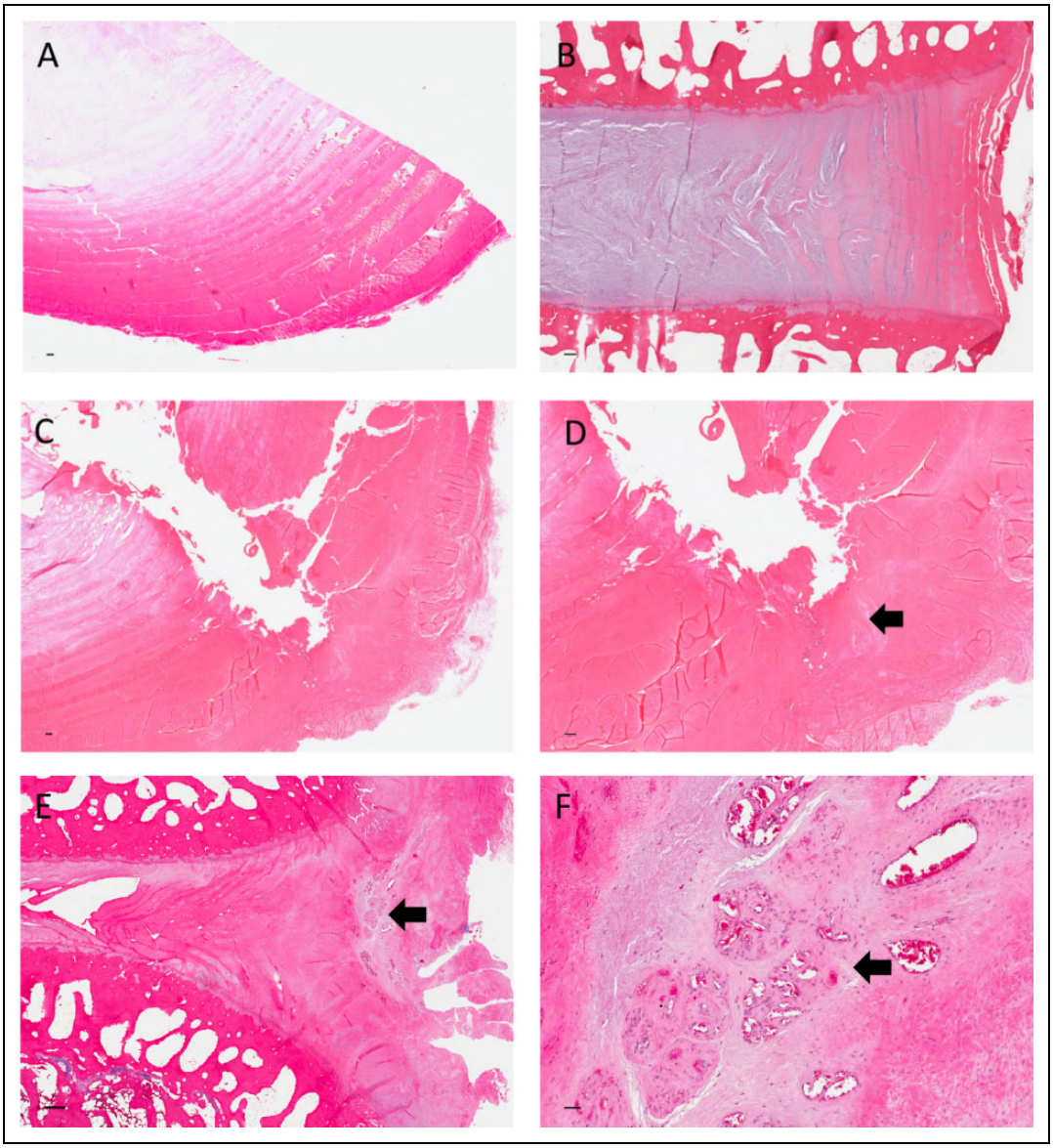

Figure 7. Sections stained with hematoxylin and eosin. (A) Control disc (axial section) demonstrating intact annulus fibrosus and adjacent nucleus pulposus. (B) Control disc (coronal section) demonstrating the coronal plane. (C) Drill-injured disc demonstrating disruption of the annulus fibrous extending into the nucleus. (D) Drill-injured disc under higher power demonstrating superficial localized fibrosis (arrow) at external annulus fibrosus with minimal vascular infiltration. (E) APN-injured disc demonstrating extensive lamellae disruption and vascular infiltration. (F) APN-injured disc demonstrating lamellar structure under high-power magnification with evidence of marked vascular invasion (arrow). Scale bar = 200 μm. APN, annulotomy and partial nucleotomy.

absent from the DBI discs. Vascular invasion is consistent with histological observations from herniated and degenerate intervertebral discs in the clinical context.[52,53] In addition, the APN-injured discs demonstrated disorganization of the lamella pattern of the AF and adjacent NP. In contrast, the DBI disc demonstrated a focal lesion with minimal disruption of the AF and NP. The absence of significant tissue ingrowth observed in DBI specimens is in agreement with the lack of a significant increase in collagen content in the DBI AF.

There are, however, important differences between these preclinical models and the human intervertebral disc that contribute to the limitations of this study. A limitation common to large animal models of intervertebral disc degeneration is the inability to assess low back pain. The only animal models allowing for low back pain assessment are rodent models.[54,55] Such models present challenges with regard to their differences to the human disc in size, anatomy, the presence of notochordal cells, and ultimately, translatability. Furthermore, in the clinical situation, the underlying disc demonstrates preexisting degeneration culminating in disc prolapse and neural compression. The models we present are of normal intervertebral discs subjected to injury to induce intervertebral disc degeneration. Discs with preexisting degeneration may have reduced capacity to repair or regenerate or may demonstrate a higher extent of

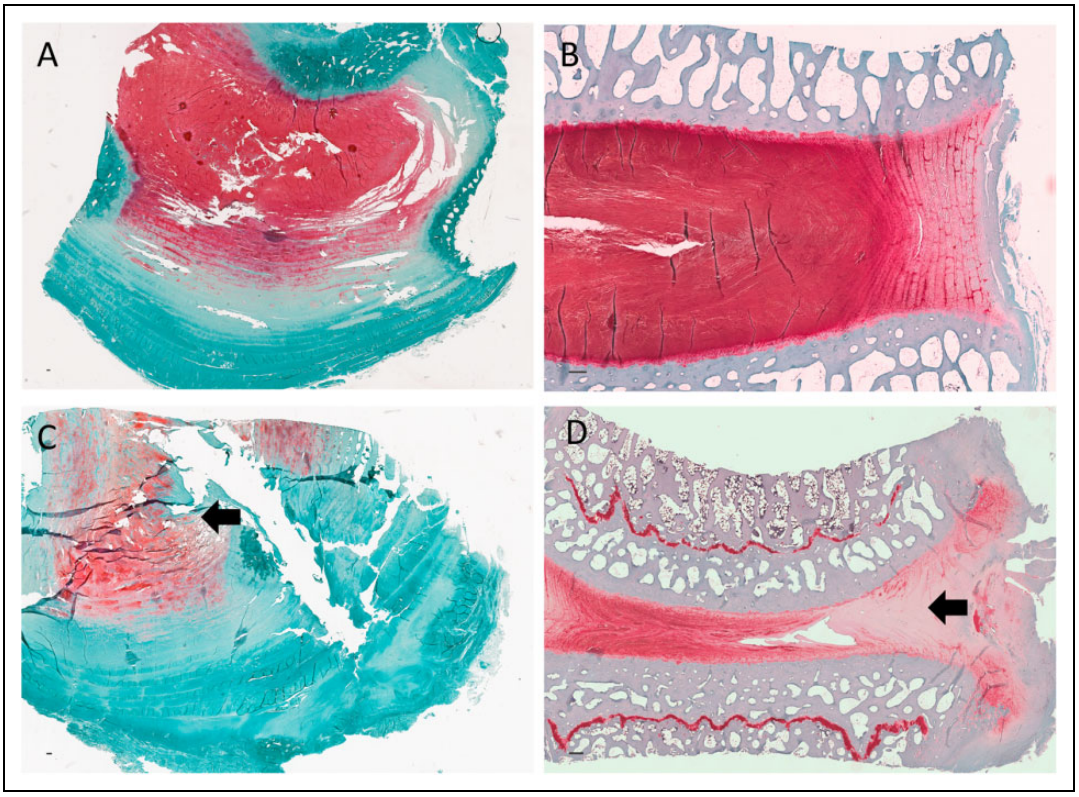

Figure 8. Sections stained with Safranin O and Fast Green. (A) Control disc (axial section) demonstrating intact annulus fibrosus and adjacent nucleus pulposus. (B) Control disc (coronal section) demonstrating the coronal plane. (C) Drill-injured disc demonstrating reduced Safranin O stain (indicative of reduced proteoglycan content) in the drill-injured region of the nucleus pulposus (arrow). (D) APN-injured disc demonstrating significant reduction in Safranin O stain in the injured region of the intervertebral disc (arrow). Scale bar = 200 μm. APN, annulotomy and partial nucleotomy).

degeneration following injury induction than the previously healthy discs included in this trial. This is an important consideration in the context of investigating regenerative therapies for disc degeneration in the future.

Conclusion

The ovine intervertebral disc drill bit and APN injury models both produce intervertebral disc degeneration at 6 months following injury. However, the severity of degeneration associated with the APN model was greater, as assessed by MRI, gross morphology, biochemical and histological analysis, than the drill bit model. Moreover, the ovine APN injury model better replicated the postdiscectomy lumbar intervertebral disc mechanistically and importantly, more closely reproduced the known pathology of disc tissues examined post–human disc herniation.[52,53]

On the basis of the aforementioned findings, we concluded that the ovine APN model provides a more suitable animal model for the evaluation of novel cellular modalities that targeted disc repair than the drill bit model. In this regard, we have subsequently used the ovine APN model of microdiscectomy to compare the relative efficacy of 2 mesenchymal stem cell preparations in their ability to restore disc integrity 6 months postsurgery.[26]

Declaration of Conflicting Interests

The author(s) declared no potential conflicts of interest with respect to the research, authorship, and/or publication of this article.

Funding

The author(s) disclosed receipt of the following financial support for the research, authorship, and/or publication of this article: Dr Chris D. Daly is the recipient of the Royal Australasian College of Surgeons Foundation for Surgery Richard Jepson Scholarship.

References

1. Hoy D, March L, Brooks P, et al. The global burden of low back pain: estimates from the Global Burden of Disease 2010 study. *Ann Rheum Dis*. 2014;73:968-974. doi:10.1136/annrheumdis-2013-204428.
2. Luoma K, Riihimäki H, Luukkonen R, Raininko R, Viikari-Juntura E, Lamminen A. Low back pain in relation to lumbar disc degeneration. *Spine (Phila Pa 1976)*. 2000;25:487-492.
3. Parker SL, Xu R, McGirt MJ, Witham TF, Long DM, Bydon A. Long-term back pain after a single-level discectomy for radiculopathy: incidence and health care cost analysis. *J Neurosurg Spine*. 2010;12:178-182. doi:10.3171/2009.9.SPINE09410.
4. Weinstein JN, Tosteson TD, Lurie JD, et al. Surgical vs nonoperative treatment for lumbar disk herniation: the Spine Patient

Outcomes Research Trial (SPORT): a randomized trial. *JAMA*. 2006;296:2441-2450. doi:10.1001/jama.296.20.2441.
5. Parker SL, Mendenhall SK, Godil SS, et al. Incidence of low back pain after lumbar discectomy for herniated disc and its effect on patient-reported outcomes. *Clin Orthop Relat Res*. 2015;473: 1988-1999. doi:10.1007/s11999-015-4193-1.
6. McGirt MJ, Ambrossi GL, Datoo G, et al. Recurrent disc herniation and long-term back pain after primary lumbar discectomy: review of outcomes reported for limited versus aggressive disc removal. *Neurosurgery*. 2009;64:338-344. doi:10.1227/01.NEU.0000337574.58662.E2.
7. Heindel P, Tuchman A, Hsieh PC, et al. Reoperation rates after single-level lumbar discectomy. *Spine (Phila Pa 1976)*. 2017;42: E496-E501. doi:10.1097/BRS.0000000000001855.
8. Daly C, Ghosh P, Jenkin G, Oehme D, Goldschlager T. A review of animal models of intervertebral disc degeneration: pathophysiology, regeneration, and translation to the clinic. *Biomed Res Int*. 2016;2016:5952165. doi:10.1155/2016/5952165.
9. Oehme D, Ghosh P, Shimmon S, et al. Mesenchymal progenitor cells combined with pentosan polysulfate mediating disc regeneration at the time of microdiscectomy: a preliminary study in an ovine model. *J Neurosurg Spine*. 2014;20:657-669. doi:10.3171/2014.2.SPINE13760.
10. Hohaus C, Ganey TM, Minkus Y, Meisel HJ. Cell transplantation in lumbar spine disc degeneration disease. *Eur Spine J*. 2008; 17(suppl 4):492-503. doi:10.1007/s00586-008-0750-6.
11. Stern WE, Coulson WF. Effects of collagenase upon the intervertebral disc in monkeys. *J Neurosurg*. 1976;44:32-44. doi:10.3171/jns.1976.44.1.0032.
12. Acosta FL Jr, Metz L, Adkisson HD, et al. Porcine intervertebral disc repair using allogeneic juvenile articular chondrocytes or mesenchymal stem cells. *Tissue Eng Part A*. 2011;17: 3045-3055. doi:10.1089/ten.tea.2011.0229.
13. Oehme D, Ghosh P, Goldschlager T, et al. Radiological, morphological, histological and biochemical changes of lumbar discs in an animal model of disc degeneration suitable for evaluating the potential regenerative capacity of novel biological agents. *J Tissue Sci Eng*. 2015;6:153. doi:10.4172/2157-7552.1000153.
14. Osti OL, Vernon-Roberts B, Fraser RD. 1990 Volvo Award in experimental studies. Anulus tears and intervertebral disc degeneration. An experimental study using an animal model. *Spine (Phila Pa 1976)*. 1990;15:762-767.
15. Melrose J, Shu C, Young C, et al. Mechanical destabilization induced by controlled annular incision of the intervertebral disc dysregulates metalloproteinase expression and induces disc degeneration. *Spine (Phila Pa 1976)*. 2012;37:18-25. doi:10.1097/BRS.0b013e31820cd8d5.
16. Goldschlager T, Rosenfeld JV, Ghosh P, et al. Cervical interbody fusion is enhanced by allogeneic mesenchymal precursor cells in an ovine model. *Spine*. 2011;36:615-623. doi:10.1097/BRS.0b013e3181dfcec9.
17. Goldschlager T, Ghosh P, Zannettino A, et al. A comparison of mesenchymal precursor cells and amnion epithelial cells for enhancing cervical interbody fusion in an ovine model. *Neurosurgery*. 2011;68:1025-1034. doi:10.1227/NEU.0b013e31820d5375.
18. Goldschlager T, Ghosh P, Zannettino A, et al. Cervical motion preservation using mesenchymal progenitor cells and pentosan polysulfate, a novel chondrogenic agent: preliminary study in an ovine model. *Neurosurg Focus*. 2010;28:E4. doi:10.3171/2010.3.FOCUS1050.
19. Melrose J, Burkhardt D, Taylor TK, et al. Calcification in the ovine intervertebral disc: a model of hydroxyapatite deposition disease. *Eur Spine J*. 2009;18:479-489. doi:10.1007/s00586-008-0871-y.
20. Hunter CJ, Matyas JR, Duncan NA. Cytomorphology of notochordal and chondrocytic cells from the nucleus pulposus: a species comparison. *J Anat*. 2004;205:357-362. doi:10.1111/j.0021-8782.2004.00352.x.
21. Wilke HJ, Kettler A, Claes LE. Are sheep spines a valid biomechanical model for human spines? *Spine (Phila Pa 1976)*. 1997; 22:2365-2374.
22. Ghosh P, Wu J, Shimmon S, Zannettino AC, Gronthos S, Itescu S. Pentosan polysulfate promotes proliferation and chondrogenic differentiation of adult human bone marrow-derived mesenchymal precursor cells. *Arthritis Res Ther*. 2010;12:R28. doi:10.1186/ar2935.
23. Zhang Y, Drapeau S, An HS, Markova D, Lenart BA, Anderson DG. Histological features of the degenerating intervertebral disc in a goat disc-injury model. *Spine (Phila Pa 1976)*. 2011;36: 1519-1527. doi:10.1097/BRS.0b013e3181f60b39.
24. Oehme D, Goldschlager T, Rosenfeld J, et al. Lateral surgical approach to lumbar intervertebral discs in an ovine model. *ScientificWorldJournal*. 2012;2012:873726. doi:10.1100/2012/873726.
25. Lim KZ, Daly CD, Ghosh P, et al. Ovine lumbar intervertebral disc degeneration model utilizing a lateral retroperitoneal drill bit injury. *J Vis Exp*. 2017;(123). doi:10.3791/55753.
26. Daly CD, Ghosh P, Zannettino ACW, et al. Mesenchymal progenitor cells primed with pentosan polysulfate promote lumbar intervertebral disc regeneration in an ovine model of microdiscectomy. *Spine J*. 2018;18:491-506. doi:10.1016/j.spinee.2017.10.008.
27. Oehme D, Ghosh P, Goldschlager T, et al. Reconstitution of degenerated ovine lumbar discs by STRO-3-positive allogeneic mesenchymal precursor cells combined with pentosan polysulfate. *J Neurosurg Spine*. 2016;24:715-726. doi:10.3171/2015.8.SPINE141097.
28. Burkhardt D, Hwa SY, Ghosh P. A novel microassay for the quantitation of the sulfated glycosaminoglycan content of histological sections: its application to determine the effects of diacerhein on cartilage in an ovine model of osteoarthritis. *Osteoarthritis Cartilage*. 2001;9:238-247. doi:10.1053/joca.2000.0381.
29. Farndale RW, Buttle DJ, Barrett AJ. Improved quantitation and discrimination of sulphated glycosaminoglycans by use of dimethylmethylene blue. *Biochim Biophys Acta*. 1986;883: 173-177.
30. Stegemann H, Stalder K. Determination of hydroxyproline. *Clin Chim Acta*. 1967;18:267-273.
31. Vergroesen PP, Kingma I, Emanuel KS, et al. Mechanics and biology in intervertebral disc degeneration: a vicious circle.

Osteoarthritis Cartilage. 2015;23:1057-1070. doi:10.1016/j.joca.2015.03.028.

32. Adams MA, Roughley PJ. What is intervertebral disc degeneration, and what causes it? *Spine (Phila Pa 1976)*. 2006;31:2151-2161. doi:10.1097/01.brs.0000231761.73859.2c.
33. Le Maitre CL, Pockert A, Buttle DJ, Freemont AJ, Hoyland JA. Matrix synthesis and degradation in human intervertebral disc degeneration. *Biochem Soc Trans*. 2007;35(pt 4):652-655. doi:10.1042/BST0350652.
34. Urban JP, Roberts S. Degeneration of the intervertebral disc. *Arthritis Res Ther*. 2003;5:120-130. doi:10.1186/ar629.
35. Elliott DM, Yerramalli CS, Beckstein JC, Boxberger JI, Johannessen W, Vresilovic EJ. The effect of relative needle diameter in puncture and sham injection animal models of degeneration. *Spine (Phila Pa 1976)*. 2008;33:588-596. doi:10.1097/BRS.0b013e318166e0a2.
36. Freemont AJ. The cellular pathobiology of the degenerate intervertebral disc and discogenic back pain. *Rheumatology (Oxford)*. 2009;48:5-10. doi:10.1093/rheumatology/ken396.
37. Natarajan RN, Andersson GB, Patwardhan AG, Verma S. Effect of annular incision type on the change in biomechanical properties in a herniated lumbar intervertebral disc. *J Biomech Eng*. 2002;124:229-236. doi:10.1115/1.1449906.
38. Hoogendoorn RJ, Wuisman PI, Smit TH, Everts VE, Helder MN. Experimental intervertebral disc degeneration induced by chondroitinase ABC in the goat. *Spine (Phila Pa 1976)*. 2007;32:1816-1825. doi:10.1097/BRS.0b013e31811ebac5.
39. Omlor GW, Nerlich AG, Wilke HJ, et al. A new porcine in vivo animal model of disc degeneration: response of anulus fibrosus cells, chondrocyte-like nucleus pulposus cells, and notochordal nucleus pulposus cells to partial nucleotomy. *Spine (Phila Pa 1976)*. 2009;34:2730-2739. doi:10.1097/BRS.0b013e3181b723c9.
40. Melrose J, Roberts S, Smith S, Menage J, Ghosh P. Increased nerve and blood vessel ingrowth associated with proteoglycan depletion in an ovine annular lesion model of experimental disc degeneration. *Spine (Phila Pa 1976)*. 2002;27:1278-1285.
41. Benoist M. The natural history of lumbar disc herniation and radiculopathy. *Joint Bone Spine*. 2002;69:155-160.
42. Lipson SJ, Muir H. Experimental intervertebral disc degeneration: morphologic and proteoglycan changes over time. *Arthritis Rheum*. 1981;24:12-21.
43. Dolan P, Adams MA. Recent advances in lumbar spinal mechanics and their significance for modelling. *Clin Biomech (Bristol, Avon)*. 2001;16(suppl 1):S8-S16. doi:10.1016/S0268-0033(00)00096-6.
44. Panjabi MM, Krag MH, Chung TQ. Effects of disc injury on mechanical behavior of the human spine. *Spine (Phila Pa 1976)*. 1984;9:707-713.
45. Shu CC, Smith MM, Smith SM, Dart AJ, Little CB, Melrose J. A histopathological scheme for the quantitative scoring of intervertebral disc degeneration and the therapeutic utility of adult mesenchymal stem cells for intervertebral disc regeneration. *Int J Mol Sci*. 2017;18:E1049. doi:10.3390/ijms18051049.
46. Griffith JF, Wang YX, Antonio GE, et al. Modified Pfirrmann grading system for lumbar intervertebral disc degeneration. *Spine (Phila Pa 1976)*. 2007;32:E708-E712. doi:10.1097/BRS.0b013e31815a59a0.
47. Blumenkrantz G, Zuo J, Li X, Kornak J, Link TM, Majumdar S. In vivo 3.0-tesla magnetic resonance T1ρ and T2 relaxation mapping in subjects with intervertebral disc degeneration and clinical symptoms. *Magn Reson Med*. 2010;63:1193-1200. doi:10.1002/mrm.22362.
48. Pennicooke B, Hussain I, Berlin C, et al. Annulus fibrosus repair using high-density collagen gel: an in vivo ovine model. *Spine (Phila Pa 1976)*. 2018;43:E208-E215. doi:10.1097/BRS.0000000000002334.
49. Sher I, Daly CD, Goldschlager T, Oehme D, Chandra RV, Ghosh P. 9.4 T MRI complements the Pfirrmann grade through better differentiation of the NP/AF. *Global Spine Congress Milan*. 2017. [TNJ: Unable to find]
50. Johannessen W, Auerbach JD, Wheaton AJ, et al. Assessment of human disc degeneration and proteoglycan content using T1ρ-weighted magnetic resonance imaging. *Spine (Phila Pa 1976)*. 2006;31:1253-1257. doi:10.1097/01.brs.0000217708.54880.51.
51. Takaishi H, Nemoto O, Shiota M, et al. Type-II collagen gene expression is transiently upregulated in experimentally induced degeneration of rabbit intervertebral disc. *J Orthop Res*. 1997;15:528-538. doi:10.1002/jor.1100150408.
52. Freemont AJ, Peacock TE, Goupille P, Hoyland JA, O'Brien J, Jayson MI. Nerve ingrowth into diseased intervertebral disc in chronic back pain. *Lancet*. 1997;350:178-181. doi:10.1016/S0140-6736(97)02135-1.
53. Doita M, Kanatani T, Harada T, Mizuno K. Immunohistologic study of the ruptured intervertebral disc of the lumbar spine. *Spine (Phila Pa 1976)*. 1996;21:235-241.
54. Lai A, Moon A, Purmessur D, et al. Assessment of functional and behavioral changes sensitive to painful disc degeneration. *J Orthop Res*. 2015;33:755-764. doi:10.1002/jor.22833.
55. Millecamps M, Czerminski JT, Mathieu AP, Stone LS. Behavioral signs of axial low back pain and motor impairment correlate with the severity of intervertebral disc degeneration in a mouse model. *Spine J*. 2015;15:2524-2537. doi:10.1016/j.spinee.2015.08.055.